Supplemental Materials

PRMT4 facilitates white adipose tissue browning and thermogenesis by methylating PPARγ

Short title: PRMT4 promotes WAT browning

Yi Zhong, Yilong Wang, Xiaoguang Li, Haojie Qin, Shu Yan, Caijun Rao, Di Fan, Duqiu Liu, Fei Deng, Yanli Miao, Ling Yang, Kai Huang

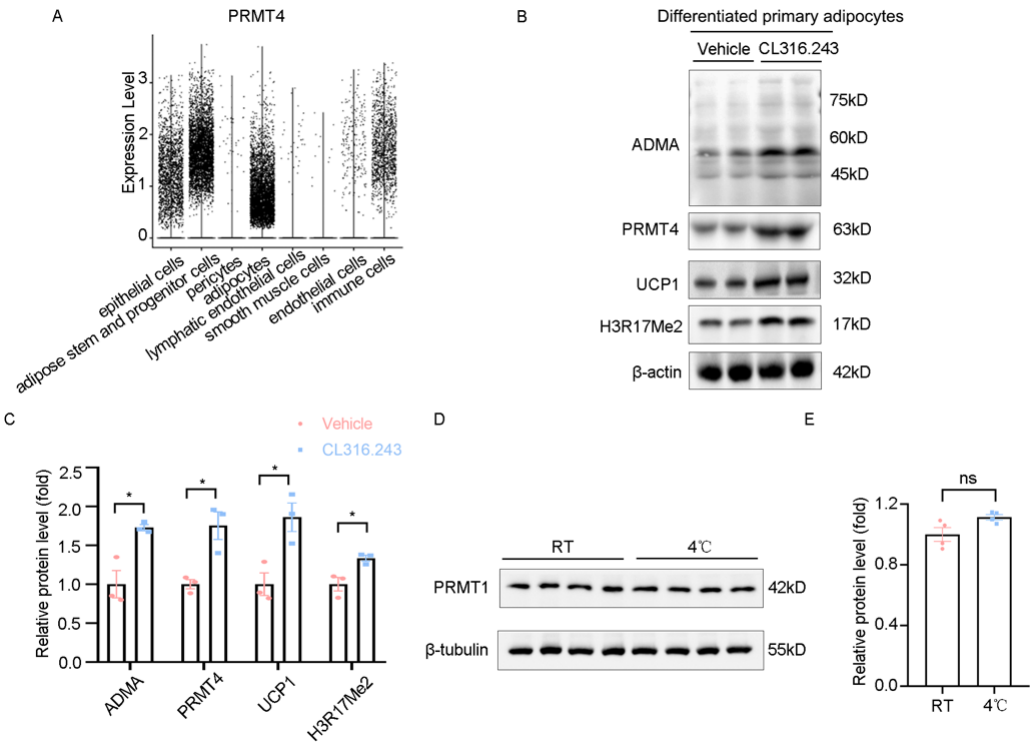

Supplemental Fig. 1

Levels of PRMT4 but not that of PRMT1 increased during iWAT browning.

A, Expression level of PRMT4 in each cell type of subcutaneous adipose tissue. **B,** SVF cells were isolated from iWAT of C57BL/6J mice and differentiated for 6 days into mature adipocytes, and then treated with CL316,243 (2 μM) for 4 h before harvested. Representative immunoblotting images of the expression levels of ADMA, PRMT4, UCP1, and H3R17Me2 in the differentiated primary adipocytes. **C,** Quantitative analysis of the protein level of ADMA, PRMT4, UCP1, and H3R17Me2 in panel B. **D,** Representative immunoblotting images displaying the expression levels of PRMT1 in iWAT from mice hosted at RT or 4 °C for 24 h. **E,** Quantitative analysis of the protein level of PRMT1 in panel D. Data are presented as mean ± SEM. **P*<0.05, ns, non-significant.

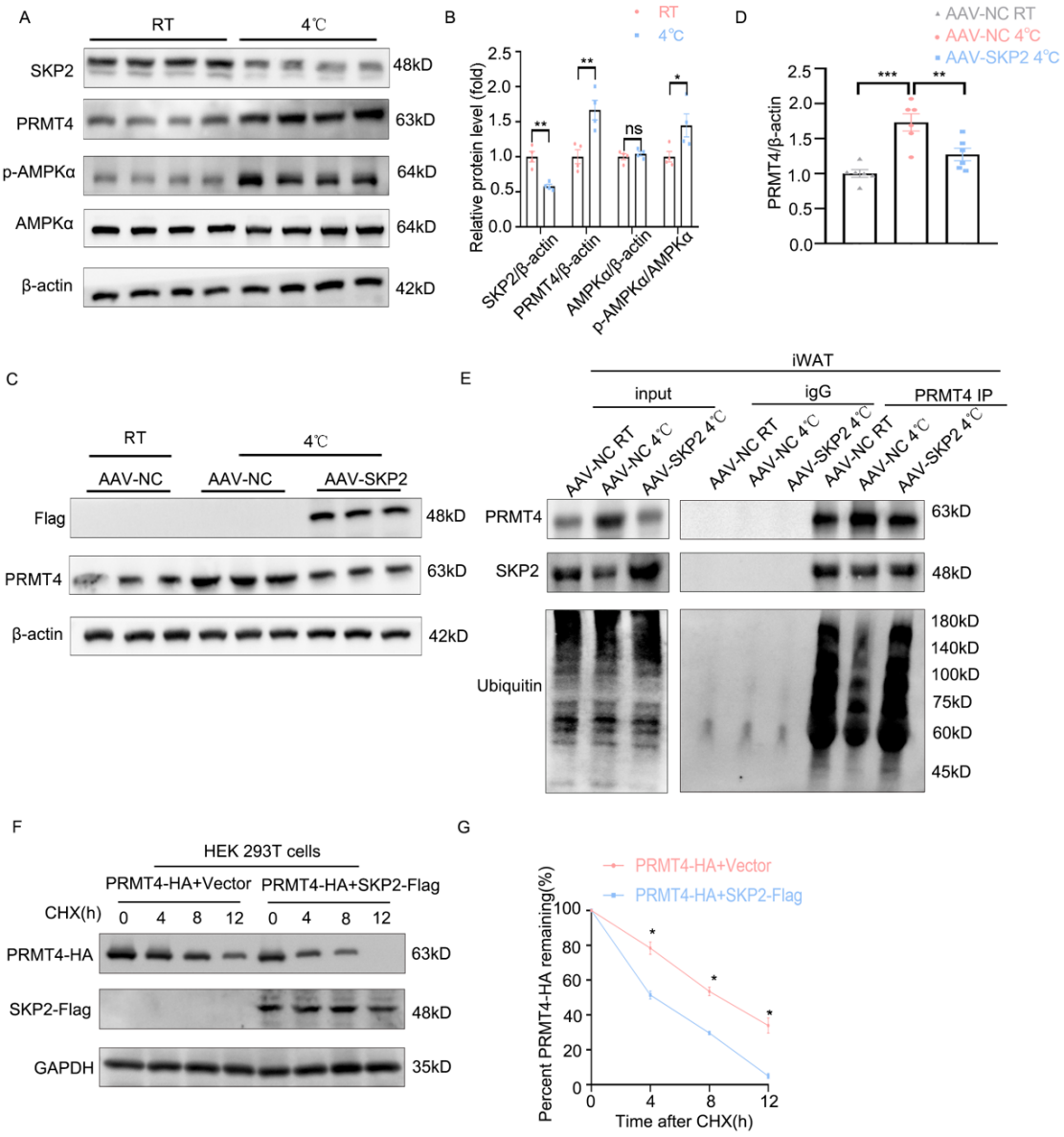

Supplemental Fig. 2

AMPKα-SKP2 axis was responsible for PRMT4 accumulation in thermogenic program.

A, Representative immunoblotting images of the expression levels of SKP2, PRMT4, p-AMPKα, and AMPKα in iWAT from mice hosted at RT or 4 °C for 24 h. **B,** Quantitative analysis of SKP2 and PRMT4 protein level as well as AMPKα phosphorylation in panel A. **C,** AAV-NC or AAV-SKP2 were subcutaneously injected vinto the bilateral inguinal areas, and mice were subjected to cold exposure (4°C) for

24 h before sacrifice. Representative immunoblotting images of the expression levels of Flag-tagged SKP2 and PRMT4 in iWAT. **D,** Quantitative analysis of the protein level of PRMT4 in panel C. **E,** Ubiquitination level of PRMT4 in iWAT following AAV-NC or AAV-SKP2 injection under RT or cold exposure. **F,** Effect of SKP2 on the stability of PRMT4. Treatment of HEK293T cells stably expressing PRMT4-HA with or without SKP2-Flag overexpression using 100 μM cycloheximide (CHX) for the indicated time. The indicated proteins were measured by immunoblotting. **G,** Quantitative analysis of the protein level of PRMT4-HA in panel F. Data are presented as mean ± SEM. **P*<0.05, ***P*<0.01 and ****P*<0.001. ns, non-significant.

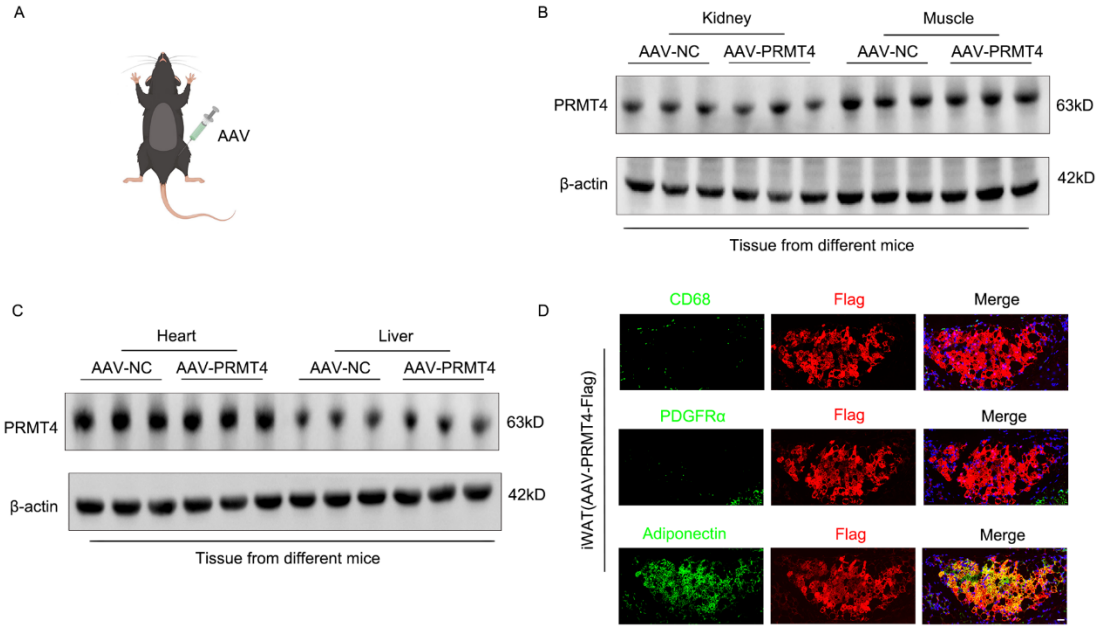

Supplemental Fig. 3

Specific overexpression of PRMT4 in iWAT.

A, Schematic diagram of local AAV injection subcutaneously into the bilateral

inguinal areas. **B-C,** Representative immunoblotting images of the expression level of PRMT4 in the indicated tissues from C57BL/6J mice after injection of AAV-NC or AAV-PRMT4 in iWAT. β-actin protein was used as the loading control. **D,** Representative immunofluorescence images for Flag (red), CD68 (macrophage marker, green), PDGFRα (preadipocyte marker, green), and Adiponectin (adipocyte marker, green) in iWAT after injection of AAV-PRMT4-Flag. Nuclei staining by DAPI (blue). Scale bar, 20 μm.

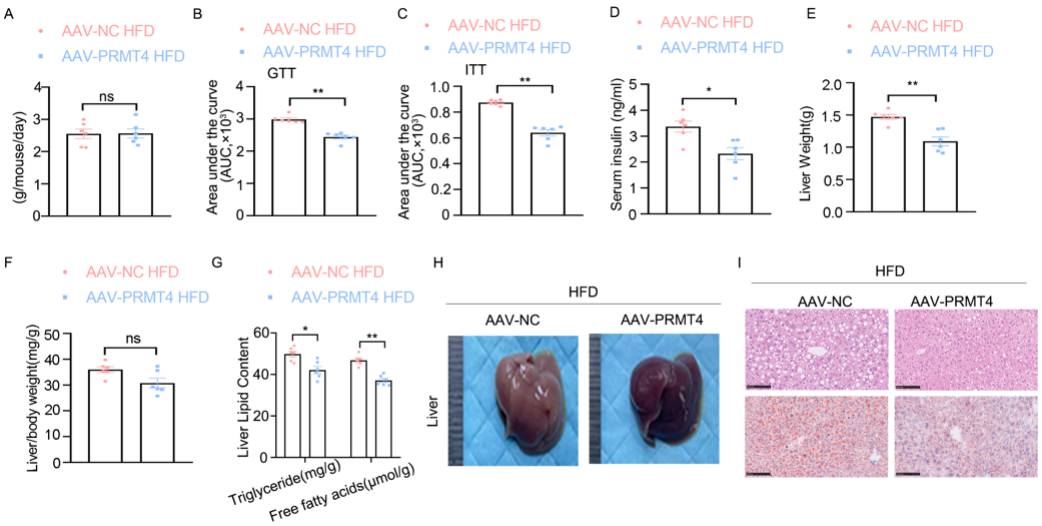

Supplemental Fig. 4

PRMT4 overexpression in iWAT meliorates diet-induced liver lipid accumulation. AAV-NC or AAV-PRMT4 was subcutaneously injected into the bilateral inguinal areas, two weeks later, the mice received 8 weeks of HFD. **A,** Food intake of the mice. **B,** Quantitative analysis of glucose tolerance test (GTT). **C,** Quantitative analysis of insulin tolerance test (ITT). **D,** Fasting serum insulin levels after 8 weeks of HFD. **E,** Liver weights of mice after 8 weeks of HFD. **F,** Liver/body weight ratio of mice after 8 weeks of HFD. **G,** Liver lipid content (triglycerides and free fatty acids) in mice. **H,** Gross morphology of the liver from mice after 8 weeks of HFD. **I,** Representative H&E

and Oil Red O staining of livers from mice after 8 weeks of HFD. Scale bar, 100 μm. Data are presented as mean ± SEM. *P<0.05 and **P<0.01. ns, non-significant.

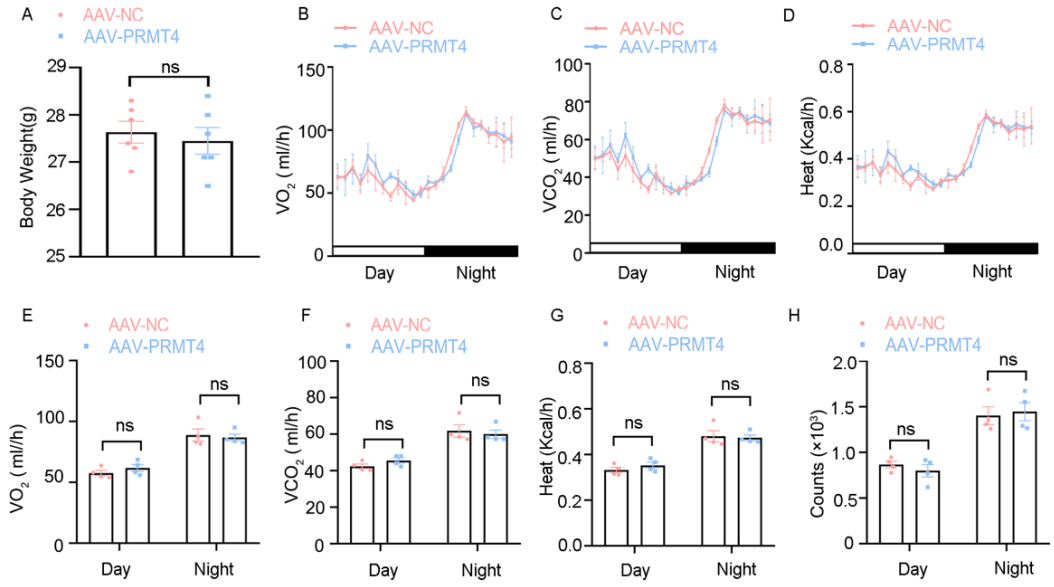

Supplemental Fig. 5

PRMT4 overexpression did not affect energy consumption at RT.

AAV-NC or AAV-PRMT4 were subcutaneously injected via the bilateral inguinal areas. **A,** Body weight of the mice was recorded. The whole-body oxygen consumption rate (VO_2) (ml/h) (**B**), carbon dioxide production (VCO_2) (ml/h) (**C**), and heat production (**D**) of mice were measured using Columbus Oxymax metabolic chambers at RT. The day/night bar represents a 12 h duration. **E,** Quantitative analysis of VO_2 in panel B. **F,** Quantitative analysis of VCO_2 in panel C. **G,** Quantitative analysis of heat production in panel D. VO_2, VCO_2, and heat production were analyzed by ANCOVA with total body mass as covariate. **H,** Average physical activity for 24 h. Data are presented as mean ± SEM. ns, non-significant.

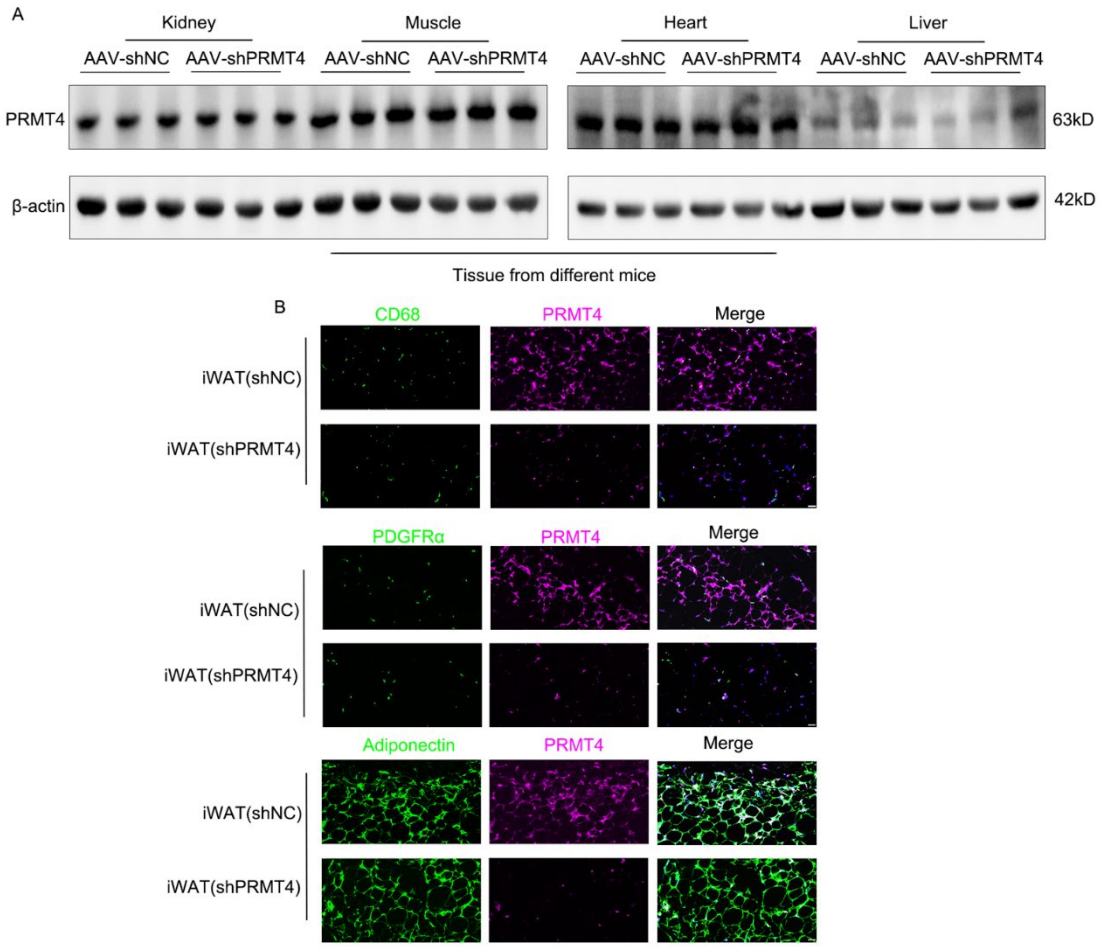

Supplemental Fig. 6

Specific knockdown of PRMT4 in iWAT.

A, Representative immunoblotting images of the expression level of PRMT4 in the indicated tissues from C57BL/6J mice with iWAT injection of AAV-shNC or AAV-shPRMT4. β-actin protein was used as the loading control. **B,** Representative immunofluorescence images for PRMT4 (purple), CD68 (macrophage marker, green), PDGFRα (preadipocyte marker, green), and Adiponectin (adipocyte marker, green) in iWAT after injection of AAV-shNC or AAV-shPRMT4. Nuclei staining by DAPI (blue). Scale bar, 20 μm.

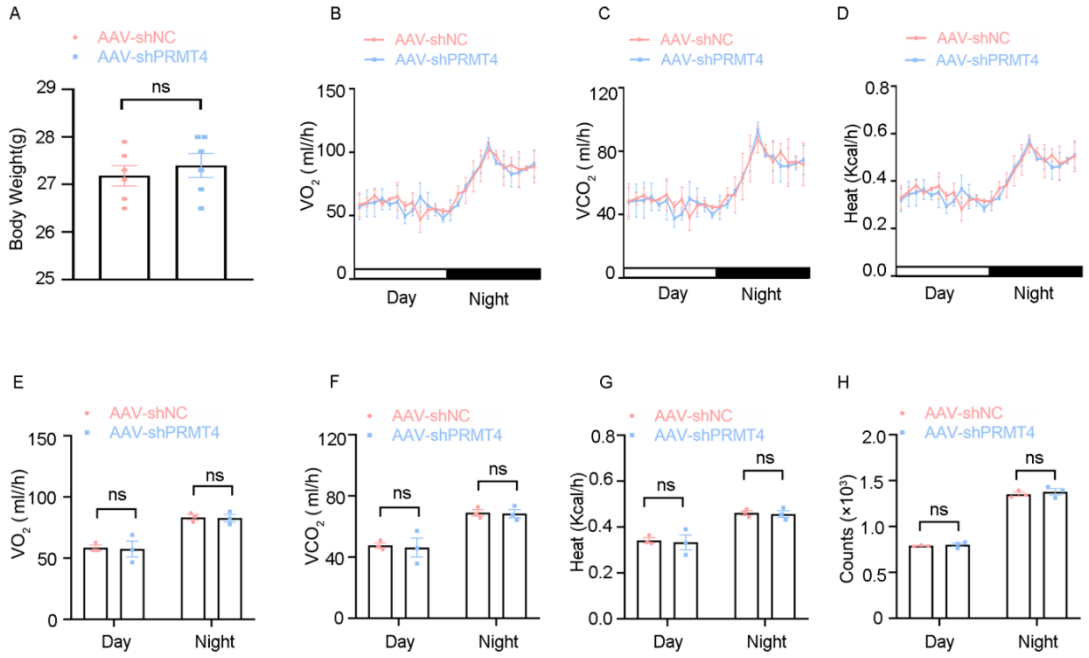

Supplemental Fig. 7

PRMT4 knockdown did not affect energy consumption at RT.

AAV-shNC or AAV-shPRMT4 were subcutaneously injected into the bilateral inguinal areas. **A,** Body weight of the mice was recorded. The whole-body oxygen consumption rate (VO_2) (ml/h) (**B**), carbon dioxide production (VCO_2) (ml/h) (**C**), and heat production (**D**) of mice were measured using Columbus Oxymax metabolic chambers at RT. The day/night bar represents a 12 h duration. **E,** Quantitative analysis of VO_2 in panel B. **F,** Quantitative analysis of VCO_2 in panel C. **G,** Quantitative analysis of heat production in panel D. VO_2, VCO_2, and heat production were analyzed by ANCOVA with total body mass as covariate. **H,** Average physical activity for 24 h. Data are presented as mean ± SEM. ns, non-significant.

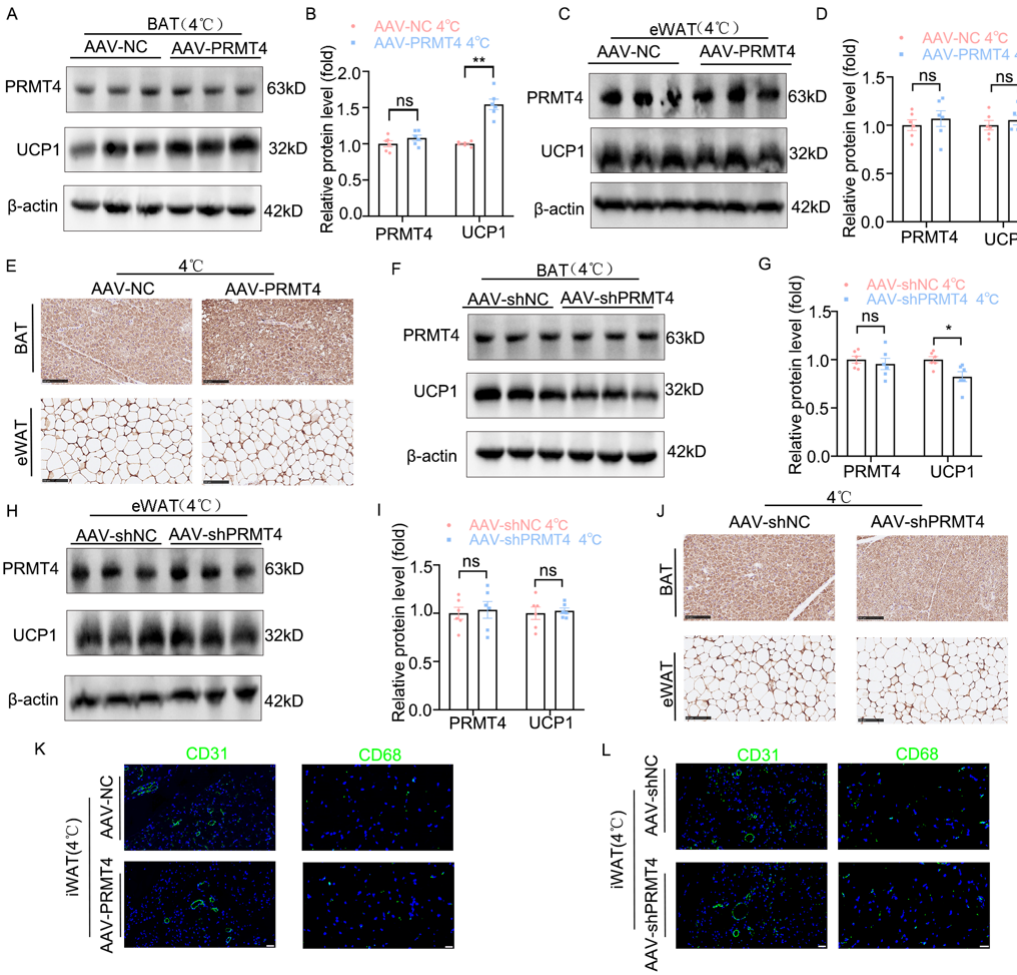

Supplemental Fig. 8

Effects of iWAT PRMT4 modulation upon BAT and eWAT thermogenic program. **A,** Representative immunoblotting images of the expression levels of PRMT4 and UCP1 in BAT. **B,** Quantitative analysis of indicated protein expression in panel A. **C,** Representative immunoblotting images of the expression levels of PRMT4 and UCP1 in eWAT. **D,** Quantitative analysis of indicated protein expression in panel C. **E,** Representative images showing UCP1 immunohistochemistry in BAT and eWAT sections. Scale bar, 100 μm. **F,** Representative immunoblotting images of the expression levels of PRMT4 and UCP1 in BAT. **G,** Quantitative analysis of indicated protein expression in panel F. **H,** Representative immunoblotting images of the expression

levels of PRMT4 and UCP1 in eWAT. **I,** Quantitative analysis of indicated protein expression in panel H. **J,** Representative images showing UCP1 immunohistochemistry in BAT and eWAT sections. Scale bar, 100 μm. **K,** Representative image showing immunofluorescence staining of CD31 (endothelial cell marker, green) or CD68 (macrophage marker, green) in iWAT with injection of AAV-NC or AAV-PRMT4 after cold exposure. Nuclei staining by DAPI (blue). Scale bar, 20 μm. **L,** Representative image showing immunofluorescence staining of CD31 (endothelial cell marker, green) or CD68 (macrophage marker, green) in iWAT with injection of AAV-shNC or AAV-shPRMT4 after cold exposure. Nuclei staining by DAPI (blue). Scale bar, 20 μm. Data are presented as mean ± SEM. *P<0.05 and **P<0.01. ns, non-significant.

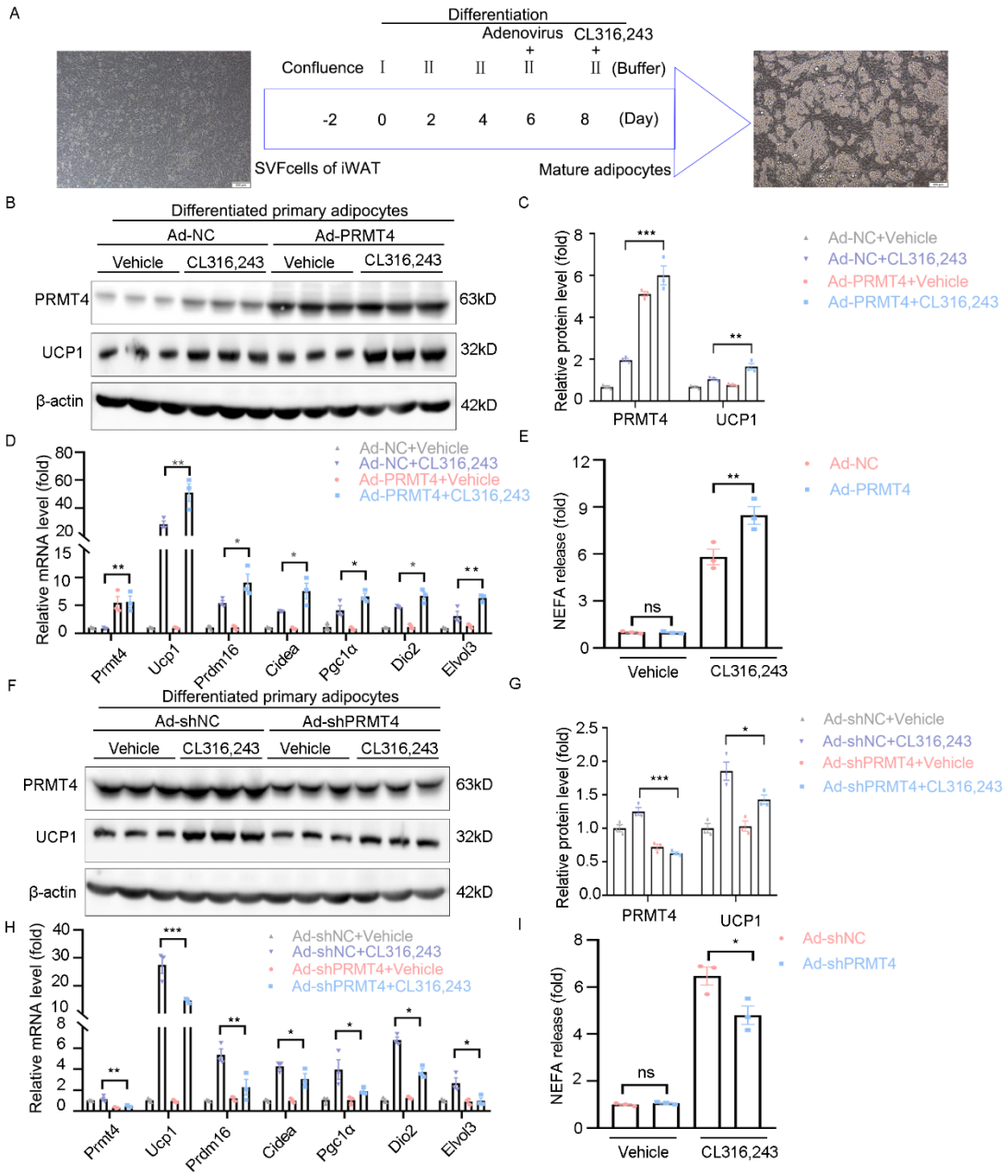

Supplemental Fig. 9

PRMT4 regulated thermogenic program of SVF cells.

SVF cells were isolated from iWAT of C57BL/6J mice and differentiated for 6 days into mature adipocytes, then the differentiated primary adipocytes were infected with the indicated adenovirus for 48 h and treated with CL316,243 (2 μM) for 4 h before harvested. **A,** Schematic illustration of in vitro differentiation of SVF cells isolated from iWAT. **B** and **F,** Representative immunoblotting images of the expression levels of

PRMT4 and UCP1 in the differentiated primary adipocytes after vehicle or CL316,243 administration. **C,** Quantitative analysis of the protein level of PRMT4 and UCP1 in panel B. **D** and **H**, Relative mRNA levels of the indicated genes in the differentiated primary adipocytes after vehicle or CL316,243 administration. **E** and **I**, Relative NEFA levels in the culture medium. **G,** Quantitative analysis of the protein level of PRMT4 and UCP1 in panel F. Data are presented as mean ± SEM. **P*<0.05, ***P*<0.01 and****P*<0.001. ns, non-significant.

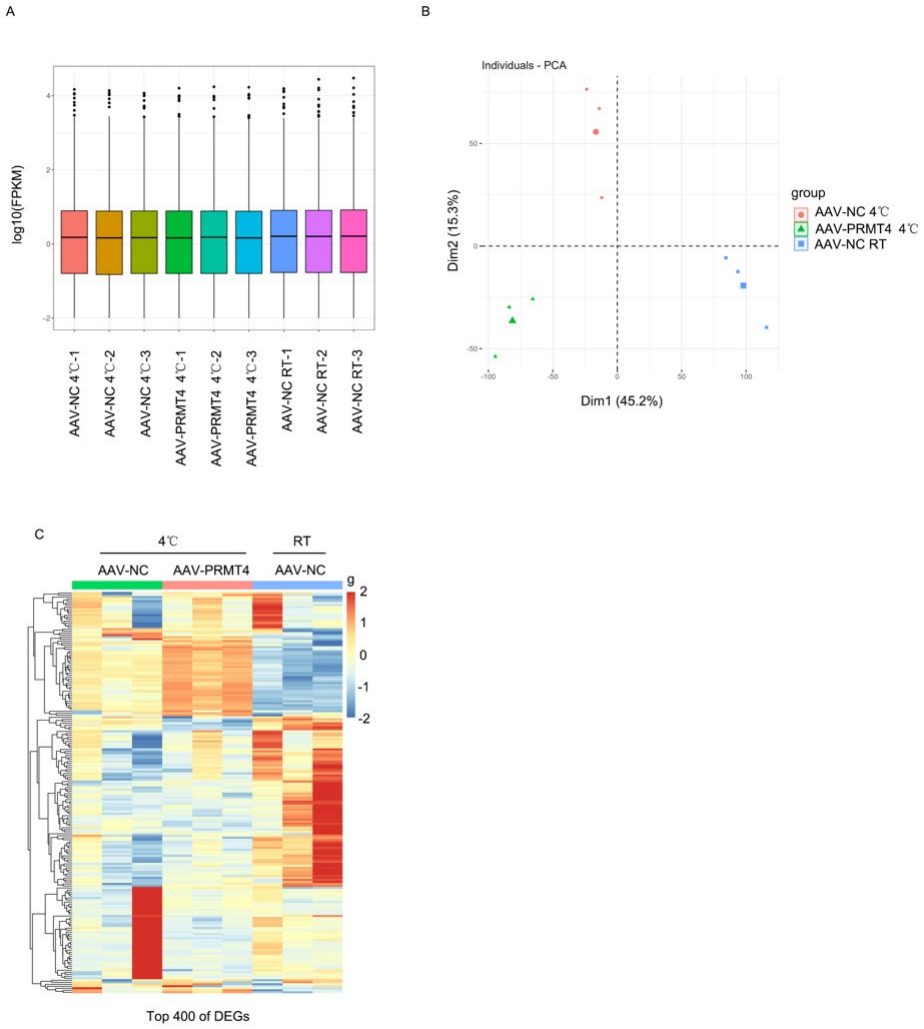

Supplemental Fig. 10

Identification of PRMT4-regulated genes by RNA-seq analysis.

A, The FPKM boxplot shows the distribution of gene expression levels among each sample. **B,** Principal component analysis (PCA) revealed global gene expression patterns upon cold stimulation or PRMT4 transduction in iWAT. **C** Hierarchical clustering revealed the top 400 differentially expressed genes (DEGs).

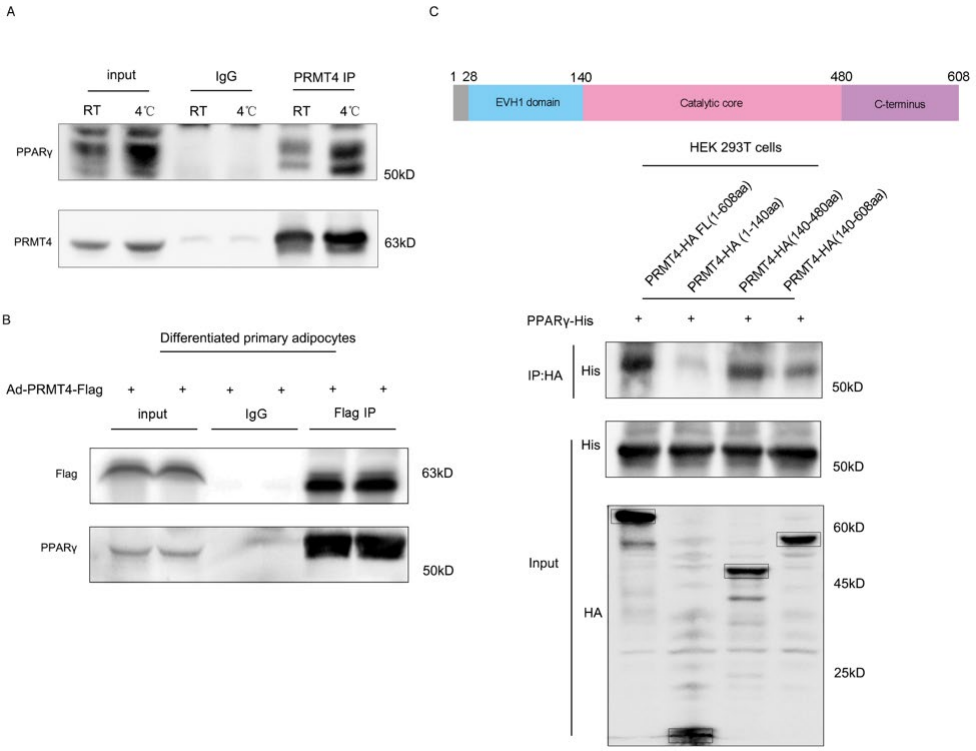

161

162 **Supplemental Fig. 11**

163 **PRMT4 interacted with PPARγ.**

164 **A,** iWAT tissues from mice were hosted at RT or 4 °C for 24 h, co-IP assay was

165 conducted. **B,** SVF cells were isolated from iWAT of C57BL/6J mice and differentiated

166 for 6 days into mature adipocytes, then the differentiated primary adipocytes were

167 infected with Ad-PRMT4-Flag for 48 h and followed by co-IP assay. **C,** The interaction

168 domains of PRMT4 with PPARγ were explored using full-length and deletion-mutated

169 PRMT4 expression constructs based on co-IP assays.

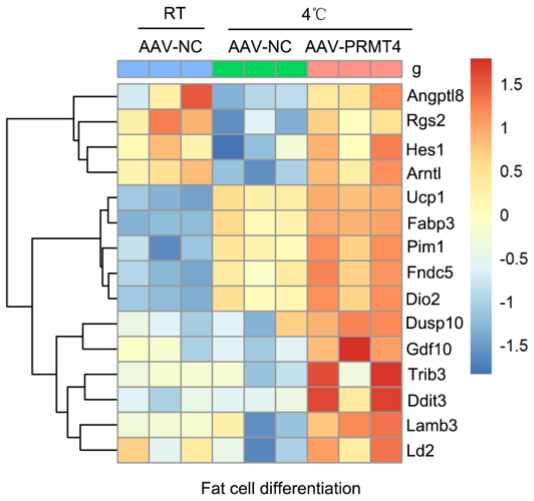

170

171 **Supplemental Fig. 12**

172 **DEGs were enriched in fat cell differentiation**

173 Fat cell differentiation-related DEGs were shown. Heatmaps represents gene

174 expression changes.

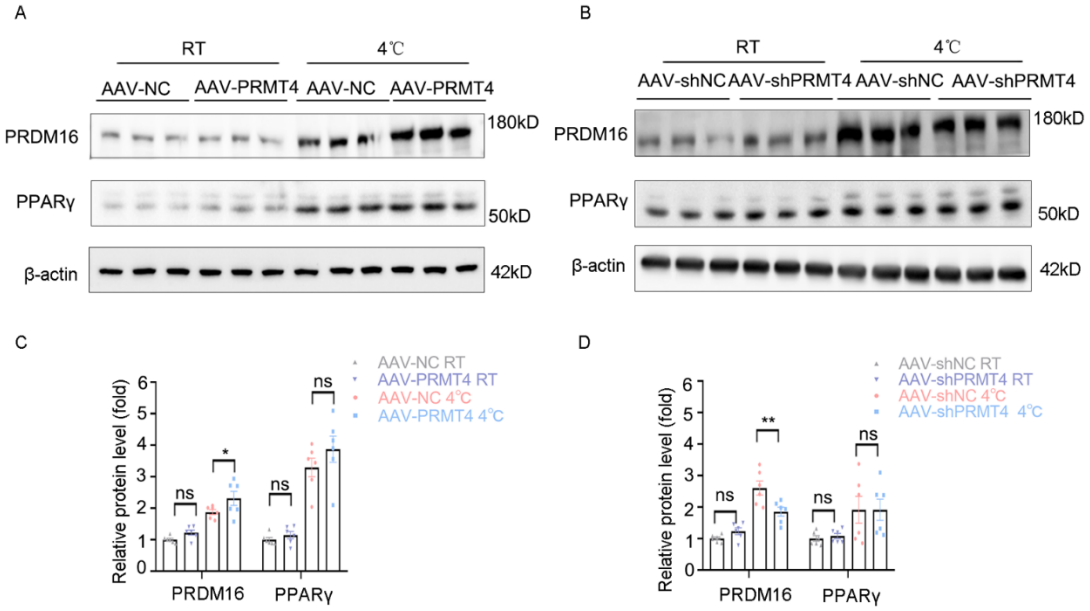

175

176 **Supplemental Fig. 13**

177 **PRMT4 regulated cold-induced PRDM16 expression in iWAT.**

178 **A, B**, Representative immunoblotting images showing the expression levels of

PRDM16 and PPARγ in iWAT from mice injected with the indicated virus subcutaneously into bilateral inguinal areas. **C-D**, Quantitative analysis of the protein level of PRDM16 and PPARγ in panel A and B. Data are presented as mean ± SEM. ***P*<0.01 and****P*<0.001, ns, non-significant.

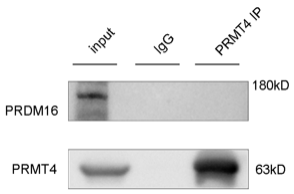

Supplemental Fig. 14

PRMT4 did not directly interact with PRDM16

Co-IP assay showed that PRMT4 did not bound to PRDM16 in iWAT.

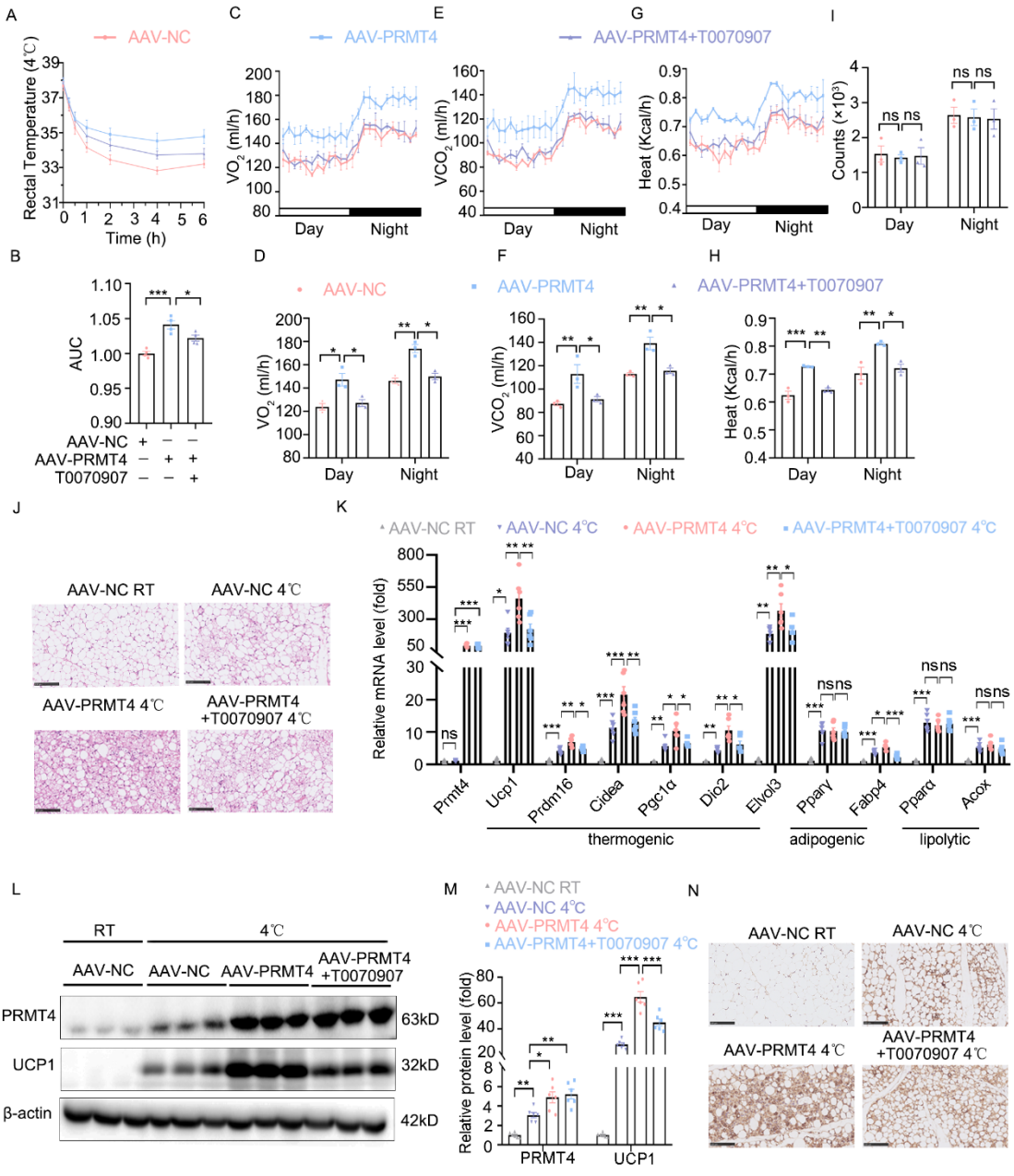

Supplemental Fig. 15

Inhibition of PPARγ by T0070907 abolishes the effect of PRMT4 on thermogenic gene expression.

A, The rectal temperature of mice during acute cold exposure (4°C) was monitored in the first 6 h. **B,** Quantitative analysis of rectal temperature in panel A. The oxygen consumption rate (VO_2) (**C**), carbon dioxide production (VCO_2) (**E**), and heat production (**G**) were analyzed. The day/night bar represents a 12 h duration. **D,**

Quantitative analysis of VO_2 in panel C. **F,** Quantitative analysis of VCO_2 in panel E. **H,** Quantitative analysis of heat production in panel G. VO_2, VCO_2, and heat production were analyzed by ANCOVA with total body mass as covariate. **I**, Average values of physical activity. **J,** Representative HE staining of iWAT sections; scale bar, 100 μm. **K,** Relative mRNA levels of thermogenic, adipogenic, and lipolytic genes. **L,** Representative immunoblotting images of the expression levels of PRMT4 and UCP1 in iWAT. **M,** Quantitative analysis of indicated protein level in panel L. **N,** Representative IHC images of UCP1 in iWAT sections were shown. Scale bar, 100 μm. Data are presented as the mean ± SEM. **P*<0.05, ***P*<0.01 and****P*<0.001. ns, non-significant.

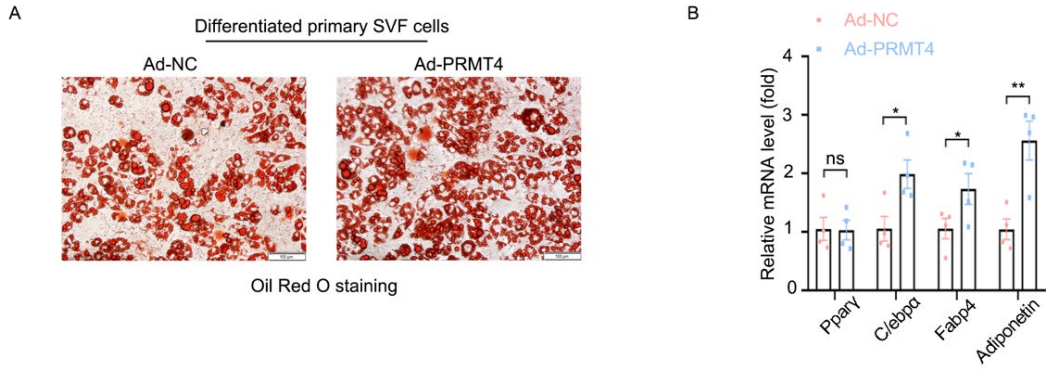

Supplemental Fig. 16

PRMT4 overexpression promotes adipogenesis in vitro.

SVF cells isolated from iWAT of C57BL/6J mice were infected with the indicated adenovirus and were then differentiated for 6 days into mature adipocytes in vitro. **A,** Representative Oil-red O staining of differentiated adipocytes on day 6. Scale bar, 100 μm. **B,** Relative mRNA levels of the indicated genes in differentiated adipocytes on day 6. Data are presented as mean ± SEM. **P*<0.05, ***P*<0.01. ns, non-significant.

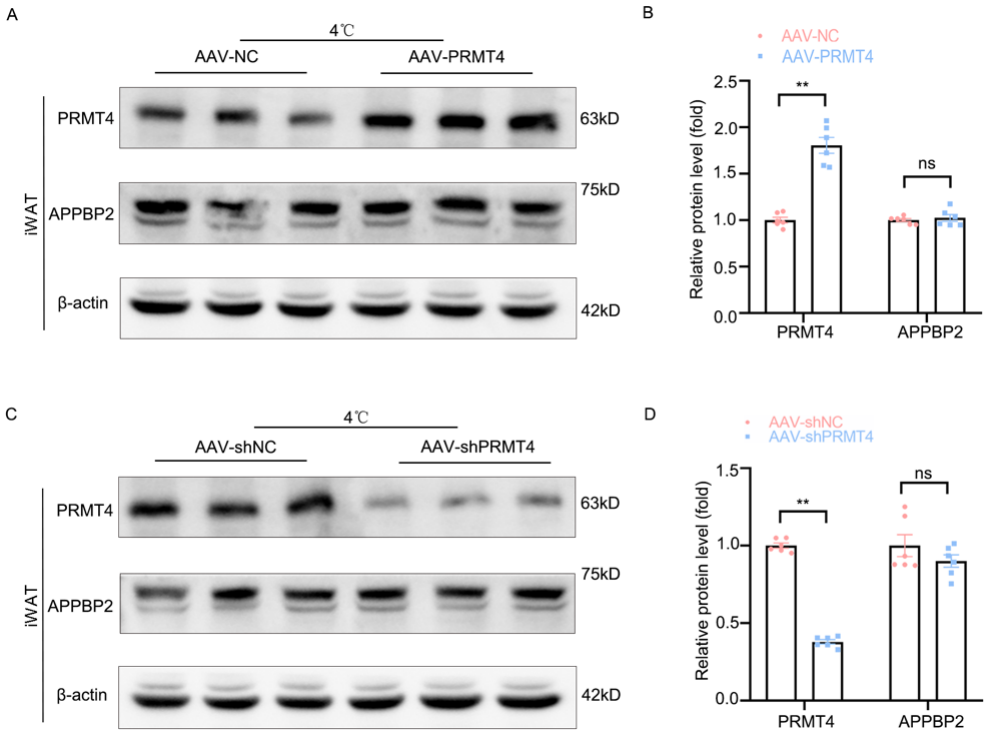

Supplemental Fig. 17

PRMT4 overexpression or knockdown did not affect protein level of APPBP2 in iWAT upon cold exposure.

AAV-NC, AAV-PRMT4, AAV-shNC or AAV-shPRMT4 was subcutaneously injected into the bilateral inguinal areas, two weeks later, mice were subjected to cold exposure (4°C) for 24 h before sacrifice. **A&C,** Representative immunoblotting images of the expression levels of PRMT4 and APPBP2 in iWAT. **B&D,** Quantitative analysis of indicated protein expression in panel A&C. Data are presented as mean ± SEM. $^{**}P<0.01$, ns, non-significant.

233 **Table S1.** Primers for qPCR

Gene	Forward 5'→3'	Reverse 5'→3'
h-β-actin	GGCACCCAGCACAATGAA	GGAAGGTGGACAGCGAGG
h-Prmt4	TCGCCACACCCAACGATTT	GTACTGCACGGCAGAAGACT
h-Ucp1	AGGTCCAAGGTGAATGCCC	TTACCACAGCGGTGATTGTTC
m-18S	TTGACGGAAGGGCACCACCAG	GCACCACCACCCACGGAATCG
m-Prmt4	TGACATCAGTATTGTGGCACAG	CTGAGGAGCCTAAGGGAATCA
m-Ucp1	AGGCTTCCAGTACCATTAGGT	CTGAGTGAGGCAAAGCTGATTT
m-Pgc1α	GGTTGAAAAAGCTTGACTGGCG	ACCAACCAGAGCAGCACACT
m-Elvol3	TTCTCACGCGGGTTAAAAATGG	TCTCGAAGTCATAGGGTTGCAT
m-Prdm16	CCAAGGCAAGGGCGAAGAA	AGTCTGGTGGGATTGGAATGT
m-Dio2	AATTATGCCTCGGAGAAGACCG	GGCAGTTGCCTAGTGAAAGGT
m-Pparα	AGAGCCCCATCTGTCCTCTC	ACTGGTAGTCTGCAAAACCAAA
m-Acox	AAATATGCCCAGGTGAAGCC	CACTGTATCGAATGGCAATGG
m-Pparγ	TCGCTGATGCACTGCCTATG	GAGAGGTCCACAGAGCTGATT
m-Fabp4	AAGGTGAAGAGCATCATAACCCT	TCACGCCTTTCATAACACATTCC
m-Adiponectin	TGTTCCTCTTAATCCTGCCCA	CCAACCTGCACAAGTTCCCTT
m-C/ebpα	CAAGAACAGCAACGAGTACCG	GTCACTGGTCAACTCCAGCAC

234